Materials Today: Proceedings 62 (2022) 2581–2586

Contents lists available at ScienceDirect

Materials Today: Proceedings

journal homepage: www.elsevier.com/locate/matpr

Turbulent flow measurements in continuous steel casting mold water model

Mirko Javurek [a,*], Markus Brummayer [b], Raimund Wincor [b]

[a] Johannes Kepler University Linz, Altenbergerstraße 69, 4040 Linz, Austria
[b] voestalpine Stahl GmbH, voestalpine-Straße 3, A-4020, Austria

ARTICLE INFO

Article history:
Received 13 December 2021
Received in revised form 17 March 2022
Accepted 28 March 2022
Available online 9 April 2022

Keywords:
Flow velocity measurement
Continuous casting steel mold
Bubbly flow
Confined jet

ABSTRACT

The flow of the liquid metal in the continuous casting process of steel is essential for process quality optimizations. Due to gas injection, a complex turbulent multiphase flow situation prevails in the mold. The high temperatures, the opacity of liquid steel and the harsh environment strongly restrict the possibilities for measurements directly in the production process. Therefore, a 1:1 scaled laboratory water model of the casting process is available at the voestalpine steel plant in order to study the flow situation. Flow measurements on this model using different methods are presented in this contribution. The results are important to understand and control the flow structure, as well as to validate mathematical models for numerical flow simulations.

1. Introduction

Austria's largest steel producing company voestalpine focusses on high quality steel strips. Therefore, a high effort in the optimization of the production process is required. One key aspect for the product quality is the continuous strand casting process, where liquid metal flows continuously into the mold and starts to solidify at the cooled mold walls (Fig. 1). The proper design and control of the turbulent liquid steel flow pattern, including the influence of inert gas bubbles resulting from a gas injection in the entry nozzle, is known to influence the produced steel quality. Due to the high temperatures and the harsh environment, the flow situation can only be studied experimentally in laboratory models of the casting process (e.g. [1–9]) and numerical flow simulations (e.g. [2,3,7–10]). Such numerical simulation models are expensive and challenging as the physics of turbulent multiphase flows is still not perfectly understood, and therefore, simulation models must be carefully validated by experimental results.

2. Experimental setup

For research purposes, voestalpine operates a 1:1 scale laboratory model of the continuous casting process with transparent walls and water as liquid representing the liquid steel flow (Fig. 2). The mold width used in the experiments is 1600 mm and the thickness is 285 mm. The submerged entry nozzle (SEN) has an inner diameter of 70 mm and the upper edge of the outlet ports is submerged 150 mm. While in the real process, the liquid steel throughput through the entry nozzle is determined by the casting speed of the solidifying strand, a pump controlled by a flow meter regulates the throughput in the water model. In order to obtain the same flow velocities in the water model, the volumetric throughput of the pump control is set to the cross section of the mold multiplied by the casting speed, which is 0.02 ms^{-1} for the presented results. Adjusting the same fluid velocity in the real process and the water model, both Reynolds and Froude similarity are fulfilled, which guaranties a similarity of the model to the real process with respect to turbulence and free surface elevations. Gas is injected inside the mold entry nozzle in the real process as well as in the model setup. The gas injection rate is increased in the water model by factor 6 in comparison to the real process in order to consider the thermal expansion of the gas when it enters the liquid steel. The injected gas forms bubbles that are carried with the liq-

Abbreviations: PIV, particle image velocimetry; SEN, submerged entry nozzle; 2D, two dimensional; SAS, scale adaptive simulation.

* Corresponding author.

https://doi.org/10.1016/j.matpr.2022.03.605
2214-7853/

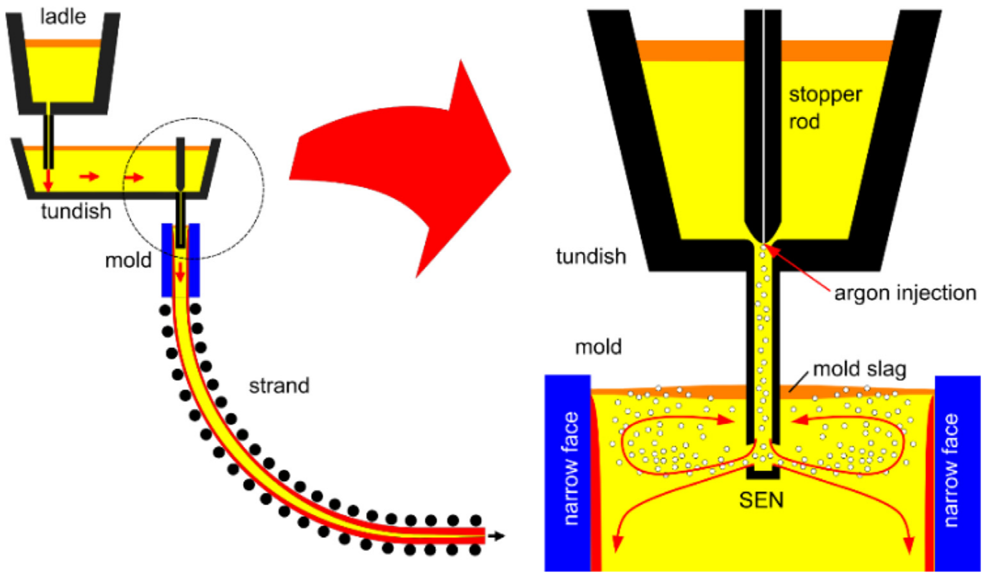

Fig. 1. Continuous steel casting process: overview (left), detail mold flow (right) with submerged entry nozzle (SEN), yellow: liquid steel. (For interpretation of the references to color in this figure legend, the reader is referred to the web version of this article.)

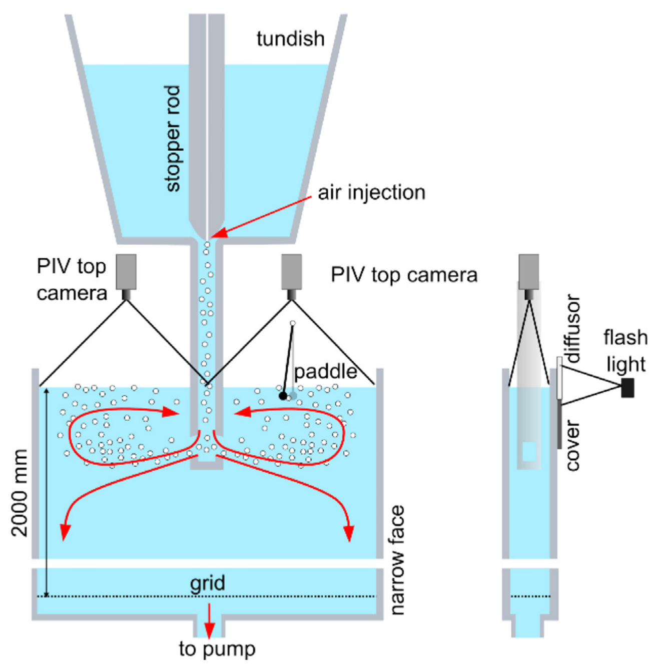

Fig. 2. Laboratory water model with measurement facilities, front and side view of the mold.

uid into the mold, where they rise to the surface and influence the liquid flow due to the buoyancy force acting on the bubbles and the resulting drag force acting on the liquid.

2.1. PIV flow measurement

For the 2D PIV method, a plane of a transparent flow medium seeded with optical tracer particles is illuminated. Two subsequent pictures are taken to calculate the 2D velocity field form the displacement of the tracer particles in between the two pictures. Due to the high density of bubbles in the water model mold flow, the transparency is lost and the PIV method can only be applied for measurement planes inside the mold, like e.g. the vertical symmetry plane (PIV front camera with laser sheet in Fig. 2) without or with a rather low gas injection [8]. For the gas loaded flow at typical (higher) injection rates, the top surface of the mold and the bubbles carried along with the surface flow are used to measure the surface flow velocities with PIV (top cameras in Fig. 2).

2.2. Paddle flow measurement

The paddle is a pendulum with a sphere that is submersed into the liquid. Due to the drag force acting on the sphere, the paddle is deflected approximately proportionally to the square of the flow velocity. Using a calibration measurement in a situation with known flow velocities, the flow velocity at the sphere can be calculated from the measured deflection. For the results shown in the following, the paddle is positioned in the center of the right mold surface half (refer Fig. 2). In the final setup, two paddles will be available, mounted on both sides of the mold. The use of two paddles will help identifying asymmetric flow patterns. The dynamics of these measurements is restricted to frequencies lower than the resonance frequency of the paddle. This method can also be applied in the real casting process.

2.3. Bubble size determination

Although the gas bubble size in liquid steel may be different from the bubble size in water due to the higher surface tension of liquid steel, it is important to know the bubble size in the water model for the validation of numerical simulation models, where the water model situation is simulated. Fig. 3a shows a camera image of bubbles at the ports of the submerged entry nozzle in the water model. The bubble size seems to be rather uniform around 5 to 6 mm. According the measured bubble rising velocities as a function of the bubble size in Fig. 3b, the rising velocity is almost constant for these diameters and therefore, different bubbles sizes as well as bubble breakup and coalescence effects do not need to be considered.

2.4. Gas bubble distribution

Video camera images taken with the front camera show qualitatively the distribution of the gas bubbles in the mold: in regions without bubbles, the black back wall of the mold model is visible

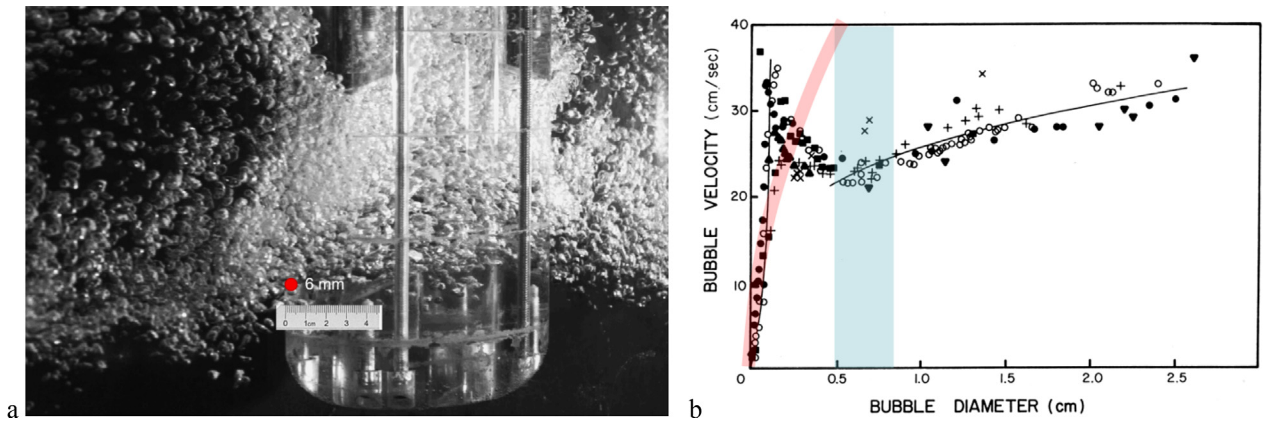

Fig. 3. a) Camera picture of gas bubbles at the ports of the submerged entry nozzle [9], b) measured bubble rising velocity as a function of the diameter after [13], red line: solid particles with same density, blue area: observed bubbles diameter range. (For interpretation of the references to color in this figure legend, the reader is referred to the web version of this article.)

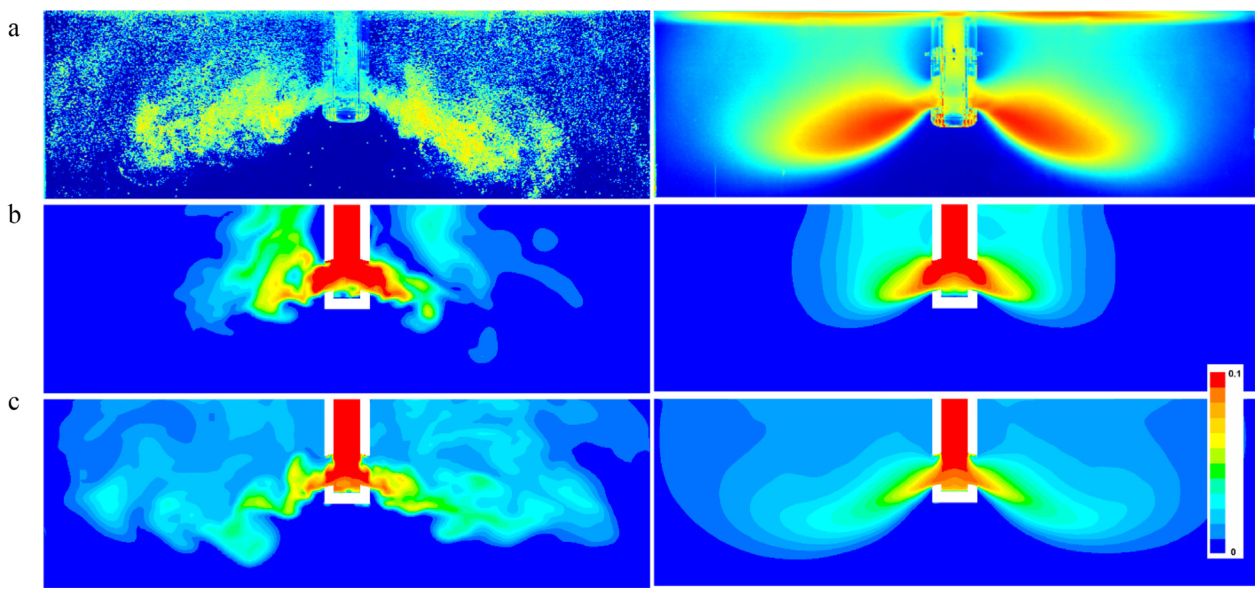

Fig. 4. Left column: instantaneous results, right column: time averaged results for a gas injection rate of 40 l min^{-1}; a) camera picture, image intensity colored with blue-green-yellow–red color scale (from dark to bright), indicating the gas bubble distribution, b) volume fraction in the center plane of simulation results without drag modification, c) with drag modification [9]. (For interpretation of the references to color in this figure legend, the reader is referred to the web version of this article.)

and the image is dark, while regions with high gas bubble load are brighter since the bubble surfaces reflect the light (Fig. 4a). Although the image density does not uniquely correspond to a gas volume fraction, it can be qualitatively compared to volume fractions from numerical flow simulations (Fig. 4b, c using the SAS turbulence model [7,9]).

The comparison shows that the gas volume fraction seems much more realistic if an increased bubble drag is used depending on the specific turbulent energy dissipation rate [9 14 15], which reduces the bubble rising velocity and transports the bubbles nearer to the small faces of the mold like observed in the camera image. Basically, a reduced bubble rising velocity could also arise from smaller bubble diameters. According to Fig. 3b, the bubble diameter needs to be less than 1 mm to cause a significant decrease of the rising velocity, which could not be observed in Fig. 3a.

3. Results

Despite of the steady boundary conditions, the turbulent flow is highly unsteady. Therefore, only time averaged results are considered in the following. Fig. 5 shows the velocity field of the top surface mold velocity field colored by the velocity component along the wide side (horizontal in the figure) from the surface center away. For lower gas injection rates, the surface flow is directed towards the center of the surface (blue = negative color range), which is known as favorable flow structure leading to a good product quality [11] and often called “double roll” flow pattern. For higher gas injection rates, the flow direction changes to “from the center away” (red color range), which is known to adversely influence the product quality (often called “single roll” flow pattern). Since the gas injection is necessary, it is essential to know the tipping point where the flow changes its direction for every combination of liquid and gas flow rate as well as for all mold dimensions and nozzle submersion depths. Despite of the symmetric geometry (the mold and nozzle geometry has two symmetry planes along the vertical center planes), the average flow pattern is asymmetric with respect to the center plane parallel to the wide face of the mold, especially for the highest gas flow rate. The reason for this asymmetry is not understood yet. Basically, asymmetric flow patterns in symmetric geometries are known to exist e.g. in

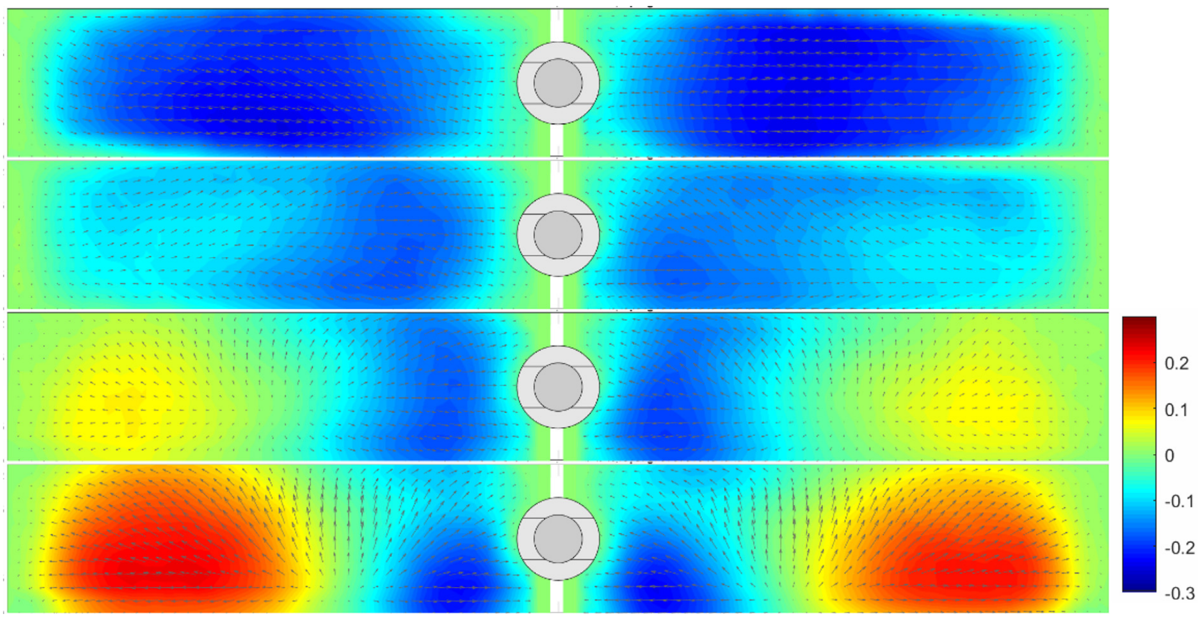

Fig. 5. Mold top surface time averaged flow velocity field (color: horizontal velocity component away from the surface center in m/s) for a constant liquid flow rate and for 5 %, 13 %, 19 % and 26 % volumetric gas flow rate (from top to bottom) in relation to volumetric liquid flow rate, measured with PIV.

diffusors, where two stable asymmetric and mirror-inverted flow patterns exist [12]. Small deviations from the symmetry of the geometry or inflow profile can trigger which of the asymmetric flow patterns establishes.

Fig. 6 shows the instantaneous velocity field at the mold level calculated by the PIV method from two subsequent camera images. During the measurement, the paddle is positioned the center of the right half of the mold top surface. Since both measurements were recorded at the same time in order to measure exactly the same flow situation, the paddle and its mounting construction obstruct some parts of the PIV surface camera picture. Therefore, the PIV field is also evaluated at surrounding (more undisturbed) locations.

Fig. 7 shows a comparison of the time averaged velocity components towards the surface center measured by the paddle (symbol: circle), and from the measured PIV field, evaluated at the paddle position (symbol: +) and surrounding positions (symbols: triangles) as a function of the gas volume injection rate in relation to the liquid flow rate for three different liquid throughput rates (given in relation to the standard throughput as used for the results in Fig. 5).

The PIV results yield systematically lower velocities than the paddle results. While the optical PIV method does not influence the flow, it could be erroneous if the bubbles on the surface used for the velocity determination do not move with the same velocity as the liquid. The paddle measures the flow velocity 40 mm below the surface. According to numerical simulations, the flow velocity at the paddle position can be around 20 % different to the surface flow velocity. Furthermore, the paddle as an intrusive method can influence the flow, and finally, it disturbs the PIV-flow velocity determination at its submersion position. Nevertheless, the discrepancies between the results of the two methods cannot by explained in detail and will be subject to further investigations. Separate measurements with both methods without interfering each other will be carried out.

The measured velocities are plotted in relation to the overall throughput. Therefore, this dimensionless velocity should be constant without gas injection if the surface velocity increases proportionally to the throughput. It is unclear whether the dimensionless velocity from the paddle measurement for 83 % liquid throughput and 0% gas injection rate is significantly higher than the other two for 0% gas injection due to non-linear effects, or if it is just a measurement error. Besides that the dimensionless velocity curves for the three different throughputs should start at the same point at 0 gas injection rate for a linear relation, it is evident that the curves diverge at increasing gas injection rates since the relative velocity between gas bubbles and liquid does not depend on the liquid

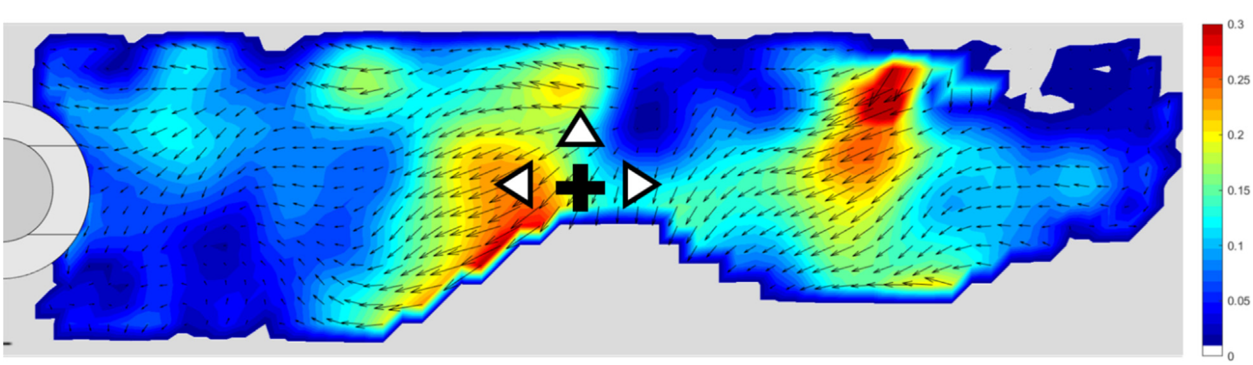

Fig. 6. Instantaneous snapshot form a PIV measurement (velocity vectors and velocity magnitude in m/s as contour plot) recorded with simultaneous paddle measurements: the + symbol marks the position where the paddle submerges into the water, while the three triangles mark surrounding positions for the comparisons in Fig. 7.

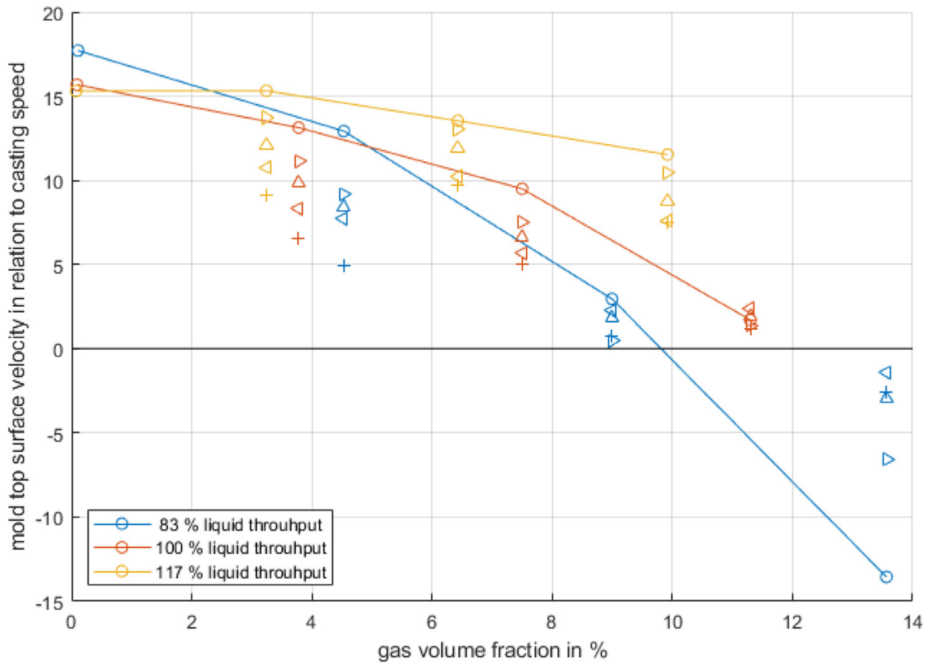

Fig. 7. Time averaged mold top surface flow velocity from paddle measurement and from PIV measurement at and around paddle position.

throughput and is therefore not proportional to the throughput. As a consequence, the gas bubble velocity field, resulting from the addition of liquid velocity field and relative bubble rising velocity field, will definitely change in a non-linear way if the liquid throughput changes, and the influence of the same gas throughput relation rate on the global flow field will be different for different liquid throughputs.

4. Conclusions

The flow measurements give valuable insight in the mold flow structure. The two measurement methods help to find out favorable flow situations and gas injection rates and serve as a validation for complex multiphase flow simulations [9]. Both measurement methods confirm that the gas injection significantly influences the mold surface flow pattern, and that the mold flow pattern can be very sensitive if the relation between gas and liquid flow rate changes. Some effects in the measurements are not fully understood, and significant differences are observed between the two mold surface velocity measurement methods. Further investigations will be carried out to resolve these shortcomings.

CRediT authorship contribution statement

Mirko Javurek: Conceptualization, Methodology, Validation, Formal analysis, Data curation, Visualization, Writing – original draft. **Markus Brummayer:** Resources, Project administration, Supervision, Funding acquisition, Writing – review & editing. **Raimund Wincor:** Resources, Investigation.

Declaration of Competing Interest

The authors declare that they have no known competing financial interests or personal relationships that could have appeared to influence the work reported in this paper.

Acknowledgements

The authors gratefully acknowledge the funding support of K1-MET GmbH, whose research program is supported by COMET (Competence Center for Excellent Technologies), the Austrian program for competence centers. COMET is funded by the Austrian ministries BMK and BMDW, the provinces of Upper Austria, Tyrol, and Styria, and the Styrian Business Promotion Agency (SFG).

Mirko Javurek reports financial support was provided by voestalpine Stahl GmbH.

References

[1] R. Sánchez-Pérez, L. García-Demedices, J.P. Ramos, M. Díaz-Cruz, R.D. Morales, Dynamics of coupled and uncoupled two-phase flows in a slab mold, Metall. Mater. Trans. B 35 (1) (2004) 85–99, https://doi.org/10.1007/s11663-004-0099-0.
[2] H. Bai, B.G. Thomas, Turbulent flow of liquid steel and argon bubbles in slide-gate tundish nozzles: Part I. model development and validation, Metall. Mater. Trans. B 32 (2001) 253–267, https://doi.org/10.1007/s11663-001-0049-z.
[3] Brian G. Thomas, Quan Yuan, Sivaraj Sivaramakrishnan, Tiebiao Shi, S.P. Vanka, Mohammad B. Assar, Comparison of Four Methods to Evaluate Fluid Velocities in a Continuous Slab Casting Mold, ISIJ International 41 (10) (2001) 1262–1271, https://doi.org/10.2355/isijinternational.41.1262.
[4] K. Timmel, N. Shevchenko, M. Röder, M. Anderhuber, P. Gardin, S. Eckert, G. Gerbeth, Visualization of Liquid Metal Two-phase Flows in a Physical Model of the Continuous Casting Process of Steel, Metall. Mater. Trans. B 46 (2) (2015) 700–710, https://doi.org/10.1007/s11663-014-0231-8.
[5] G. Gerbeth, S. Eckert, K. Timmel, T. Wondrak, Recent LIMMCAST Results on the Modeling of Steel Casting, J. Manuf. Sci. Prod. 15 (1) (2015) 131–139, https://doi.org/10.1515/jmsp-2014-0036.
[6] H. Murakawa, T. Shimizu, S. Eckert, Development of a high-speed ultrasonic tomography system for measurements of rising bubbles in a horizontal cross-section, Measurement 182 (2021) 109654, https://doi.org/10.1016/j.measurement.2021.109654.
[7] Z. Liu, B. Li, A. Vakhrushev, M. Wu, A. Ludwig, Physical and Numerical Modeling of Exposed Slag Eye in Continuous Casting Mold using Euler–Euler Approach Physical and Numerical Modeling of Exposed Slag Eye in Continuous Casting Mold using Euler-Euler Approach, Steel Res. Int. 90 (4) (2019) 1800117, https://doi.org/10.1002/srin.201800117.
[8] M. Javurek, R. Wincor, B. Kaufmann, Numerical and Experimental Study of Continuous Casting Mold Flows with High Gas Loading, Proc. STEELSIM (2005) 297–310. download at fluid.jku.at.
[9] M. Javurek, R. Wincor, Bubbly Mold Flow in Continuous Casting: Comparison of Numerical Flow Simulations with Water Model Measurements, Steel Res. Int. (2020), https://doi.org/10.1002/srin.202000415.

[10] Z. Liu, A. Vakhrushev, M. Wu, A. Kharicha, A. Ludwig, B. Li, Scale-Adaptive Simulation of Transient Two-Phase Flow in Continuous-Casting Mold, Metall. Mater. Trans. B 50 (1) (2019) 543–554, https://doi.org/10.1007/s11663-018-1443-0.

[11] S. Kunstreich, P.H. Dauby, Effect of liquid steel flow pattern on slab quality and the need for dynamic electromagnetic control in the mould, Ironmaking & Steelmaking (2005), https://doi.org/10.1179/174328105X15823.

[12] I.E. Idelchik, Handbook Of Hydraulic Resistance, 4th Revised And, Augmented Edition., Begell, New York, 2007.

[13] J. Szekely, Fluid Flow Phenomena in Metals Processing, Academic Press, 1979.

[14] F. Brucato, F. Grisafi, G. Montane, Chem. Eng. Sci. 53 (18) (1998) 3295.

[15] G.L. Lane, M.P. Schwarz, G.M. Evans, Proc. 10th European Conference on Mixing 197 (2000).